Theoretical and Computational Acoustics
D. Lee, Y-H Pao, M.H. Schultz, and Y-C Teng (Editors)

Noise Cancellation by Arrays of Active Noise Sources in Enclosures with Impedance Surfaces

G. Rosenhouse and E. Saski
Faculty of Civil Engineering, Technion-Israel Institute of Technology
Haifa, 32000, Israel

Abstract

The paper presents a new computer program for calculation and graphical display of sound fields caused by sound sources in enclosed spaces. For the simulation purposes the sources include monopoles, dipoles, quadrupoles etc as primary and secondary sources. We describe the sound field affected by rigid and absorbing boundaries, introducing the mathematical complexity due to the complex spherical wave reflection over highly absorbing areas. Next, impedance boundary effects are analyzed by an exact integral solution where necessary and in other cases by an approximate formulation based on "image" sources using complex reflection coefficients. The simulation program is then used to describe sound fields within enclosures containing a desired number of absorbing walls. Engineering and physical conclusions summarize the present work, including descriptions of the sound fields of interest.

1. Introduction

Active noise control within enclosures is involved not only with the superposition of sound fields caused by various sources, but also with reflections which add a diffusive field to the direct one. This combination increases considerably the complexity of the sound fields of both primary and secondary sources that serve the Active Noise Control (ANC). ANC is involved with multi-reflections effects not only because of the boundaries in the domain, but also due to all other obstacles in the examined environment that can be influential. Such sound reflections strongly distort the sound field in a way that might be understood only by a global view of the domain, as will be demonstrated in this paper.

There are many analysis methods for simulation of sound fields within enclosures. Basic reference books on room acoustics in this context are those of Cremer, Mueller and Schultz (1978) and Kuttruff (1976).

These methods include:

Ray tracing methods: The physical fundamentals of the methods and historical background are given in Pierce (1981). Specific publications on the use of these methods in acoustical analyses of auditoria were presented for example by Schroeder (1970), Santon (1976), Krokstad et al. (1968, 1983) and Sekiguchi, et al. (1985).

Image sources methods: Juricic and Santon (1973) and Gensane and Santon (1979). A more advanced theory, but with the deficiency of too many image sources at high order reflections was presented by Sakurai (1987), who superposed the response from reflected sounds from rigid plane panels, using the line integral formulation based on

Kirchhoff's formula and Kirchhoff's boundary conditions. Rosenhouse and Saski (1995) modified the image source method to enclosures with several sound absorbing impedance surfaces of high absorption coefficients.
Numerical techniques: Problems with complicated domains, such as obstacles within the enclosure, are more reasonably solved by numerical techniques like the Finite Element Method (FEM) combined with modal analysis, Migeot (1993) and the Boundary Element Method (BEM) for steady state and transient fields respectively - Terai, T., Kawai in the book of Ciskowski and Brebbia (1991).
Modal analysis combined with minimization: See Nelson and Elliott (1992).
In the present paper we apply the image sources method in empty rooms, where the direct sound and the effect of reflections from the wall surfaces within the enclosures are taken into account and some surfaces are highly sound absorbing. Various case studies show the possibility of using the method as an aid for design based on general understanding of source locations effect and the enclosure shape and properties. It brings us to concepts of modern control. Toady's control methodologies enable the computer "see" by guess technologies more than people can see. The computer can find today the clear picture of hidden phenomena by techniques of eliminating noise and observing meaningful clues and dots. The human brain can also draw conclusions by observing trends and clues, and even to some extent "intuition". The rest of the paper develops the technology and illustrates some sound fields created by a combination of primary and secondary sources, in various configurations, to show possibilities of active noise control in enclosures, saving a lot of computational minimization effort.

2. The choice between modal analysis based on rays reflected from impedance surfaces

A main difference between sound radiation in an enclosure and sound radiation in a free space is the existence of multi-reflections in enclosures due to the bounding surfaces, that should be considered carefully. Hence, an essential element in the analysis of a sound field in an enclosure is the reflection of sound from a sound absorbing surface. The strength and the directivity of the reflections and the natural modes of the enclosure depend on the boundary conditions that are attributed to the bounding surfaces. Both modal analysis and ray theories of room acoustics are possible and useful for different analysis purposes.
Generally, modal analysis is not common in room acoustics because of the overwhelming number of eigen frequencies and normal modes involved (about 10^9 within the audio frequency domain). This situation does not enable an adequate acoustic estimation for design purposes. To this fact one should add the difficulties due to possible complexities in the room's geometry, including coupling between rooms and surface irregularities.
The approach based on sound rays and their reflection may be considered relatively simple, and we use it to illustrate sound fields in enclosures for Active Noise Control (ANC) design. The effect of multi-reflections of sound waves from impedance surfaces and their influence on ANC was discussed in detail by Rosenhouse and Saski (1995 - Active 95) and Chapter 3. It appears that when the sound absorption coefficient of a surface is small, it is possible to use an image source, taking into account complex surface impedance and complex absorption coefficient (Ingrad and Morse, 1968), which is simple to use. On the other hand, the reflection from highly absorbing surfaces

is much more complicated and necessitates an exact solution (Thomasson, 1977). The two types of solutions will be used simultaneously in the next section in order to find a solution which is within a prescribed margin of error and also reasonably easy and convenient for use.

3. Sound fields in enclosures with impedance surfaces

A typical room consists mostly of one or two highly absorbing surfaces (walls, ceilings, floors) while the other surfaces absorb very little acoustic energy - See figure 1 for the scheme. After establishing the sound reflection model of the various kinds of surfaces of the room, the comprehensive model of the sound field analysis in enclosure can be built. That includes all the reflecting surfaces, using geometrical acoustics and application of image sources. The following assumptions on which this model is based include:

* Using the principles of geometrical acoustics, reflections of sound from rigid surfaces are considered mirror reflections. It means that instead of considering the whole reflector, image sources represent its effect on the internal sound field.
* Reflections from low absorption surfaces are included in the cases where mirror images are considered. However, under such circumstances the reflection coefficient becomes complex.
* Calculation of reflections from a highly absorbing surface can be correctly derived only by using an exact solution. The pattern of reflection from such surfaces is usually very scattered, which justifies the application of the exact solution under those conditions in spite of the significant increase in the complexity of the mathematical expressions involved.
* After a sound ray hits a highly absorbing surface, in our model the higher order reflections from the neighboring reflecting surfaces are ignored, since only an insignificant error occurs This assumption is also a condition for terminating the series of reflections. Last limitation is schematically illustrated in figure 2.

As a result of the last assumption, the sound field of a room will be derived considering first and second order image sources, in accordance with its geometry. The first model of analysis of the velocity potential ψ in the room assumes that the room surfaces are of a low absorption coefficient, which allows for application of an "approximate method" which will be described latter in this paper. Next we assume that one of the surfaces (number 1), is highly absorbent, which necessitates application of the "exact model". In our examples, the source which is located at (x_0, y_0, z_0), radiates a pure tone of 300 Hz. We assume that the velocity of sound propagation in air is 340 m/s. The room has a box shape of the dimensions X, Y, Z and a receiver is located in it at (x, y, z).

The calculation initiates with estimation of the direct radiation of sound:

$$\psi = \frac{\exp(ikR)}{4\pi R}; \quad R = \sqrt{(x-x_0)^2 + (y-y_0)^2 + (z-z_0)^2}$$

Next, reflections of the first order from the 6 reflecting surfaces n=1 are calculated:

$$\psi'_n = C_m \frac{\exp(ikR'_n)}{4\pi R'_n}; \quad n = 1,2,\ldots,6$$

$$C_m = \frac{\varsigma_n \cos(\theta_n) - 1}{\varsigma_n \cos(\theta_n) + 1}; \quad \cos(\theta_n) = \frac{h_n}{R'_n};$$

$$h_1 = z + z_0;\ h_2 = y + y_0;\ h_3 = x + x_0;\ h_4 = 2Z - z_0 - z;\ h_5 = 2Y - y_0 - y;\ h_6 = 2X - x_0 - x$$

$$R'_1 = \sqrt{(x - x_0)^2 + (y - y_0)^2 + h_1^2}; \quad R'^1_2 = \sqrt{(x - x_0)^2 + h_2^2 + (z - z_0)^2};$$

$$R'_3 = \sqrt{h_3^2 + (y - y_0)^2 + (z - z_0)^2}; \quad R'_4 = \sqrt{(x - x_0)^2 + (y - y_0)^2 + h_4^2};$$

$$R'_5 = \sqrt{(x - x_0)^2 + h_5^2 + (z - z_0)^2}; \quad R'_6 = \sqrt{h_1^2 + (y - y_0)^2 + (z - z_0)^2}$$

Now the second order reflections are calculated as already given in Rosenhouse and Saski (1995 - Active 95) and chapter 3 for reflections from two adjacent reflecting surfaces. However, when the surfaces are parallel we have two possible reflections instead of one. See figure 3. The resulting formulae are:

$$\psi''_{mn} = C'_{mn} C'_m \frac{\exp(ikR''_{mn})}{4\pi R''_{mn}}; \quad n = 1,2,\ldots,6$$

$$C'_{mn} = \frac{\varsigma_m \cos(\theta'_m) - 1}{\varsigma_m \cos(\theta'_m) + 1}; \quad C'_m = \frac{\varsigma_n \cos(\theta'_n) - 1}{\varsigma_n \cos(\theta'_n) + 1}$$

For parallel surfaces we have the following source receiver distances:

$h_{14} = 2Z - z + z_0;\ h_{25} = 2Y - y + y_0;\ h_{36} = 2X - x + x_0;$

$h_{41} = 2Z - z_0 + z;\ h_{52} = 2Y - y_0 + y;\ h_6 = 2X - x_0 + x$

The corresponding distances are:

$$R''_{12} = \sqrt{(x - x_0)^2 + h_2^2 + h_1^2}; \qquad R''_{13} = \sqrt{h_3^2 + (y - y_0)^2 + h_1^2};$$

$$R''_{14} = \sqrt{(x - x_0)^2 + (y - y_0)^2 + h_{14}^2}; \quad R''_{15} = \sqrt{h_6^2 + (y - y_0)^2 + h_1^2};$$

$$R''_{23} = \sqrt{h_3^2 + h_2^2 + (z - z_0)^2}; \qquad R''_{24} = \sqrt{(x - x_0)^2 + h_2^2 + h_4^2}$$

$$R''_{25} = \sqrt{(x - x_0)^2 + h_{25}^2 + (z - z_0)^2}; \quad R''_{26} = \sqrt{h_6^2 + h_2^2 + (z - z_0)^2};$$

$$R''_{34} = \sqrt{h_3^2 + (y - y_0)^2 + h_4^2}; \qquad R''_{35} = \sqrt{h_3^2 + h_5^2 + (z - z_0)^2};$$

$$R''_{36} = \sqrt{h_{36}^2 + (y - y_0)^2 + (z - z_0)^2}; \quad R''_{41} = \sqrt{(x - x_0)^2 + h_5^2 + h_4^2}$$

$$R''_{45} = \sqrt{(x - x_0)^2 + h_5^2 + h_4^2}; \qquad R''_{46} = \sqrt{h_6^2 + (y - y_0)^2 + h_4^2};$$

$$R''_{52} = \sqrt{(x - x_0)^2 + h_{52}^2 + (z - z_0)^2}; \quad R''_{56} = \sqrt{h_6^2 + h_5^2 + (z - z_0)^2};$$

$$R''_{63} = \sqrt{h_{63}^2 + (y - y_0)^2 + (z - z_0)^2};$$

The angles to be calculated depend on the order of reflection of the rays. This implies that we have to compare for each case the geometrical measures, D_{mn} and D^0_{mn}. Using those quantities we have for $D_{mn} > D^0_{mn}$:

$$\cos(\theta_{m'}) = \frac{h_m}{R''_{mn}} \quad \text{and} \quad \cos(\theta_n) = \frac{h_n}{R''_{mn}}$$

Otherwise:

$$\cos(\theta_{m'}) = \frac{h_n}{R''_{mn}} \quad \text{and} \quad \cos(\theta_n) = \frac{h_m}{R''_{mn}}$$

The definitions of D_{mn} and D^0_{mn} are respectively:

$$D_{12} = \frac{h_2}{h_1} z_0; D_{13} = \frac{h_3}{h_1} z_0; D_{15} = \frac{h_5}{h_1} z_0; D_{16} = \frac{h_6}{h_1} z_0$$

$$D_{23} = \frac{h_3}{h_2} z_0; D_{24} = \frac{h_4}{h_2} z_0; D_{26} = \frac{h_6}{h_2} z_0; D_{34} = \frac{h_4}{h_3} z_0$$

$$D_{35} = \frac{h_5}{h_3} z_0; D_{45} = \frac{h_5}{h_4}(Z - z_0); D_{46} = \frac{h_6}{h_4}(Z - z_0); D_{46} = \frac{h_6}{h_4}(Z - z_0); \quad \text{and}$$

$$D^0_{12} = y_0; D^0_{13} = x_0; D^0_{15} = Y - y_0; D^0_{16} = X - x_0; D^0_{23} = x_0; D^0_{24} = Z - z_0;$$

$$D^0_{26} = X - x_0; D^0_{34} = Z - z_0; D^0_{35} = Y - y_0; D^0_{45} = Y - y_0; D^0_{46} = X - x_0; D^0_{56} = X - x_0;$$

For parallel surfaces we have:

$$\cos(\theta'_m) = \cos(\theta'_n) = \frac{h_{mn}}{R''_{mn}}$$

The solution for a highly absorbent boundary (surface number 1 in figure 1 follows the exact representation - see Rosenhouse and Saski (1995 - Active 95). From figures 4, 5 we chose for illustration the situation given in figure 4. This situation yields the following expressions for calculating the resulting sound field. The total sound radiation is involved with four components of the velocity potential:

$$\psi = \psi_0 + \psi'_1 + \psi'_2 + \psi'_3$$

The first term stands for the direct radiation of sound:

$$\psi_0 = \frac{\exp(ikR)}{4\pi R}$$

The second expression is due to the first order reflection from surface 1:

$$\psi'_1 = \frac{\exp(ikR'_1)}{4\pi R'_1} + \psi_{SD} + \psi_B$$

The third expression is the first order reflection from the second surface:

$$\psi'_2 = \frac{\exp(ikR'_2)}{4\pi R'_2}$$

The last expression represents the reflection of the second order, namely:

$$\psi''_{12} = \left\{ \frac{\exp(ikR''_{12})}{4\pi R''_{12}} + \psi'_{SD} + \psi'_B \right\} C'_{r2}$$

To summarize, the reflection of sound from surface 1 is calculated following the "exact solution". In its expression, ψ_{SD} and ψ_B are terms from the solution shown by Thomasson, taking into account the effects of the real source S and its image S'_1. The reflection from surface 2 is based on the reflection coefficient C_{r2} for the incidence angle θ_2. In addition, ψ'_{SD} and ψ'_B, are the corresponding terms of the solution

presented by Thomasson, taking into account the image sources S_2' and S_{12}''. S_2' is the real source suitable for surface 1, after being reduced by the reflection coefficient C_{r2}' for the incidence angle θ_2'.

4. Examples

The aforementioned theory is used now for calculation of some examples of reflections up to the second order, as discussed below. The active control simulation is represented here by the set of secondary sources and the superposition of their fields with that of the primary source. Surface 1 in figure 1 has the following specific impedance components:

$$\Re(\varsigma) = \Im(\varsigma) = 14$$

while those surfaces of low sound absorption acquire the values:

$$\Re(\varsigma) = \Im(\varsigma) = 1000$$

Figure 6 shows the sound field of a monopole within the enclosure. A radial sound radiation pattern is observed.It is seen that the decay of sound from the source outwards is not smooth any more, but some interference obstructions appear close to the location of the source, and practically disappear at a certain distance.

Now we introduce an additional secondary monopole source in anti-phase with the primary source, as depicted in figures 7, 8, 9. In figure 7 we observe that the sound level is reduced in a strip-like domain which is normal to the axis between the sources. If the additional auxiliary source is moved closer to the primary source, as in figure 8, stronger attenuation is achieved at points which are far from both sources, and the domain of higher noise level in the vicinity of the sources becomes smaller. If the additional monopole is located apart from the primary source, as in figure 9, the sound field mapping changes significantly, but no general contribution to the noise reduction is obtained by the secondary control unit.

An introduction of secondary dipole and quadrupole sources as shown in figures 10, 11 yields a slight reduction of the levels of the primary source field at regions far from the source.

Next, we consider an addition of two secondary monopole sources in the vicinity of the primary source as in figure 12, each of half the strength of the primary source and in anti-phase to it. Once again we see that the sound field is reduced significantly.

Finally, a test of five anti-phased monopoles each with fifth the strength of the primary source were placed in the vicinity of the primary source, as in figure 13. We see that in this case the sound field is greatly attenuated. This last result is in agreement with the theoretical approach of canceling the sound field created by a primary noise source. This theory suggests that a large number of anti-phased sources of exactly the same strength as of the primary source can cancel the

5. Summary

This paper studies active noise cancellation in a typical room. Such a room consists of one or two absorbing boundaries, while the rest of the boundaries are practically not absorbing. The model is based on the following assumptions:

* Reflection from a rigid boundary is taken as an "optical" mirror reflection. Here, the common "image source" is used.

* A reflection from a boundary with a low absorption coefficient is involved with a complex reflection coefficient. Yet, a usual "image source" can replace the reflecting surface.
* A reflection from a boundary of high sound absorption coefficient necessitates an application of the "exact" solution, which is characterized by a dispersed reflection.

Some of the results are:

- When an acoustic monopole acts in a room, the radial pattern fits an omni-directional source, but it is not characterized by the ever decreasing circular domains, emanating from the source. First, the levels decrease, and then overcome a number of disturbances, to become virtually constant at a certain distance from the source.
- adding secondary sources in an anti-phase leads to the following results:
  a. The sound levels are reduced in a strip normal to the axis between the sources.
  b. If the auxiliary sources are moved to the vicinity of the primary source a significant attenuation is observed in the far sound field, and the domain of high level in the near field is significantly reduced in size.
- an introduction of a secondary dipole source and a secondary quadrupole source in the vicinity of the primary source, leads to only a slight reduction in the levels in regions which are far from the source.
- A significant reduction in the sound field is obtained by adding two secondary monopole sources which are close to the location of the primary source and are half its strength.
- five monopole sources surrounding the primary source, each with a fifth of the strength of the primary source, cause a large attenuation of the sound field. This result is close to the theoretical approach of annihilating the sound field caused by a source of noise by surrounding it with a large number of auxiliary anti-phased sources.

6. References

1. . Antes, H., Applications in environmental noise, Chapter 11 in: Ciskowski, R.D., Brebbia, C.A. (editors), Boundary Element Methods in Acoustics, Computational Mechanics Publications- Southampton and Boston and Elsevier Applied Science - London and New-York, 1991
2. Ciskowski, R.D., Brebbia, C.A. (editors), Boundary Element Methods in Acoustics, Computational Mechanics Publications- Southampton and Boston and Elsevier Applied Science - London and New-York, 1991
3. Cremer, L., Mueller, H.A., Schultz, T.J., Principles and Applications of Room Acoustics, Applied Science Publishers, London & NY, 1982, volumes 1 and 2
4. Gensane, M., Santon, F., Predicting of sound fields in rooms of arbitrary shape: validity of the image sources method, Jr. Sound Vib., 63, 1979, 97-108
5. Juricic, H., Santon, F., Images et rayons sonores dans le calcul numerique des echogrammes, Acustica, 28, 1973, 77-89
6. Krokstad, A., Strom, S., Sorsdal, S., Calculating the acoustical room response by the use of ray tracing technique, Jr. Sound Vib., 8, 1968, 118-125
7. Krokstad, A., Strom, S., Sorsdal, S., Fifteen years' experience with computerized ray tracing, Appl. Acoust., 16, 1983, 291-312
8. Kuttruff, H., Room Acoustics, Applied Science Publishers, London, 1976
9. Migeot, J.-L., Active noise control of a car interior, SYSNOISE application note 26, 19.10.1993
10. Morse, P.M., Ingrad, K.U., Theoretical Acoustics, McGraw-Hill, NY, 1968, 259 -263

11.Nelson, P.A., Elliott, S.J., Active Control of Sound, Academic Press, London, 1992
12.Pierce, A.D., Acoustics, McGraw-Hill, NY, 1981. Ch. 8: Ray acoustics
13.Rosenhouse, G., Saski, E., Noise cancellation by use of arrays of active noise sources in the vicinity of impedance surfaces, Active 95, Newport beach, CA, USA, 6.81995, 685-696
14.Santon, F., Numerical prediction of echograms and of the intelligibility of speech in rooms, Jr. Acoust. Soc. Am., 59, 1976, 1399-1405
15.Sakurai, Y., The early reflections of the impulse response in an auditorium, J. Acoust. Soc. Jpn. (E), 8, 1987, 127-138
16.Schroeder, M.R., Digital simulation of sound transmission in reverberant spaces, Jr. Acoust. Am., 47, 1970, 424-431
17.Sekiguchi, K., Kimura, S., Sugiyama, T., Approximation of impulse response through computer simulation based on finite sound ray integration, J. Acoust. Soc. Am. Jpn. (E), 6, 1985, 103-115
18.Terai, T., Kawai, Y., BEM applications in room acoustics, Chapter 10 in: Ciskowski, R.D., Brebbia, C.A. (editors), Boundary Element Methods in Acoustics, Computational Mechanics Publications- Southampton and Boston and Elsevier Applied Science - London and New-York, 1991
20..Thomasson, S.I., Reflection of waves from a point source by an impedance boundary, Jr. Acoust. Soc. Am., 59, 4, 1976, 780-785

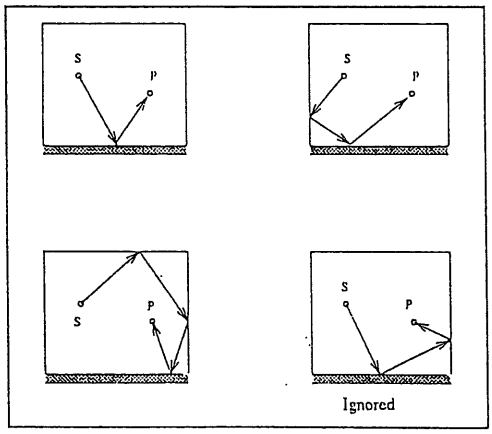

Figure 2. A model of a highly absorbing surface in a room and the relevant reflections

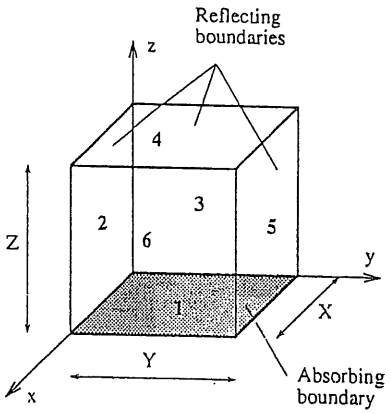

Figure 1. Configuration of a typical room

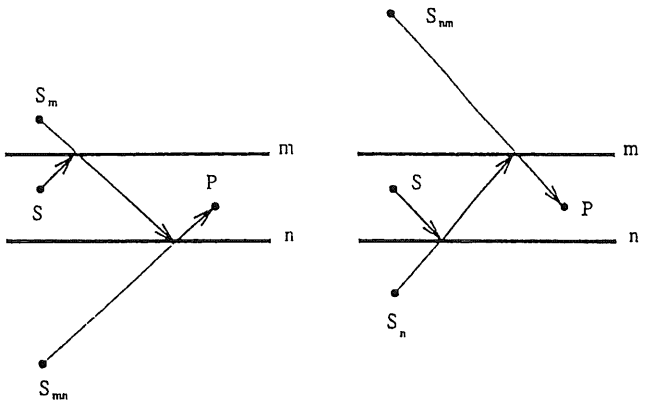

Figure 3. Two types of possible reflections between parallel walls

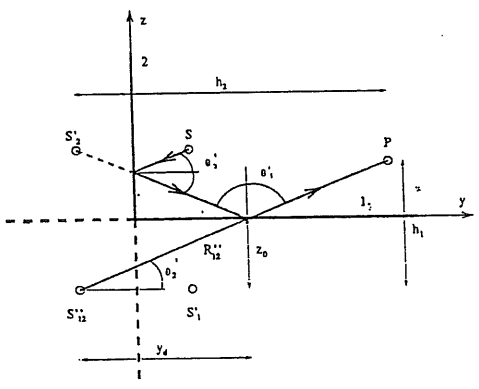

Figure 4. Second order effects: Case A

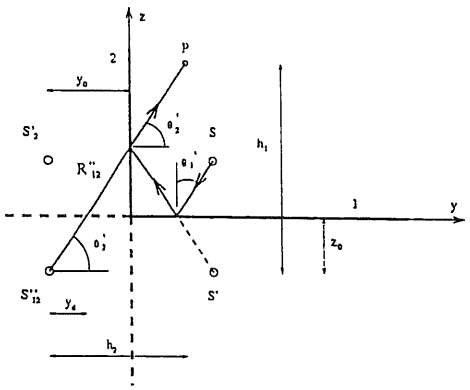

Figure 5 Second order effects: Case B

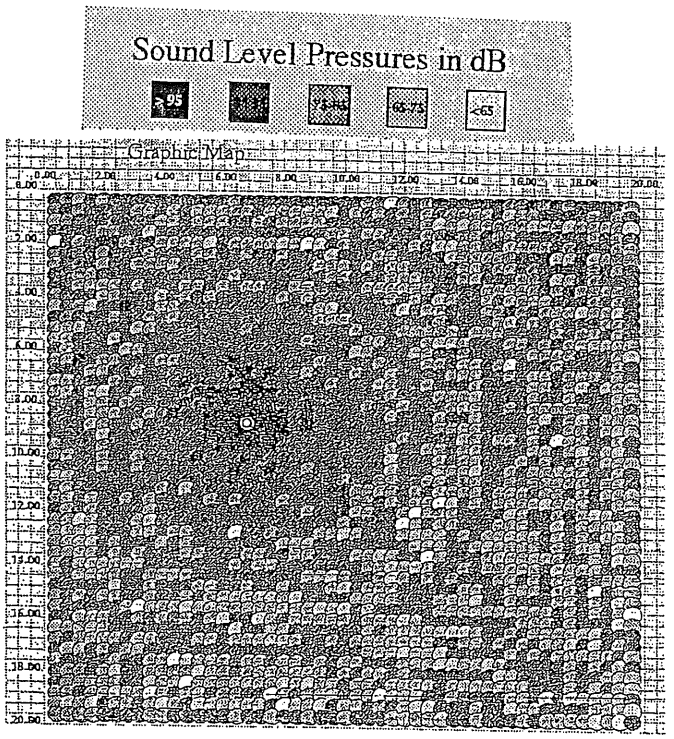

Figure 6. Primary sound field in an enclosure

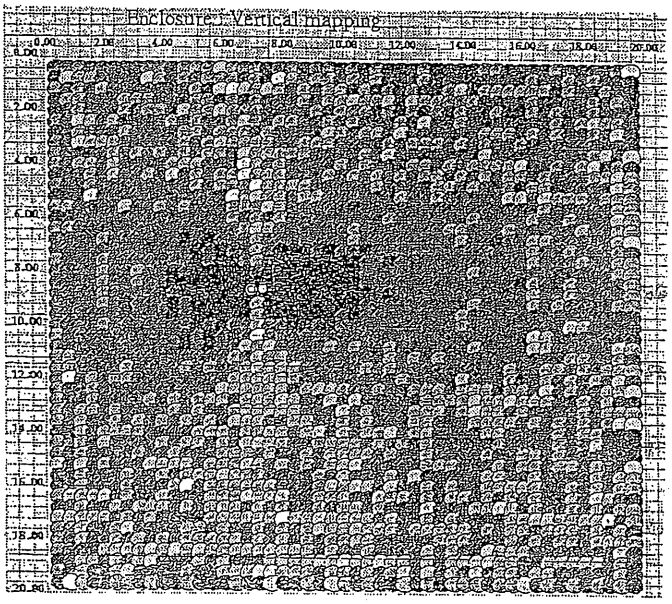

Figure 7. Sound field when a secondary monopole is close to the primary source

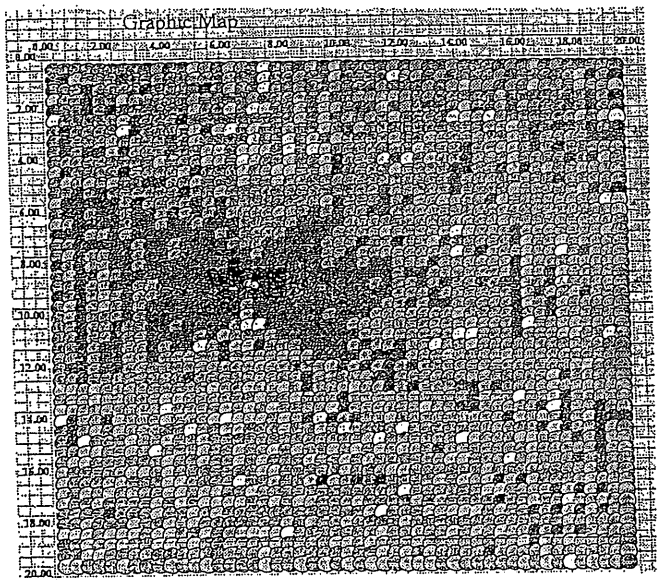

Figure 8. Sound field when a secondary monopole is very close to the primary source

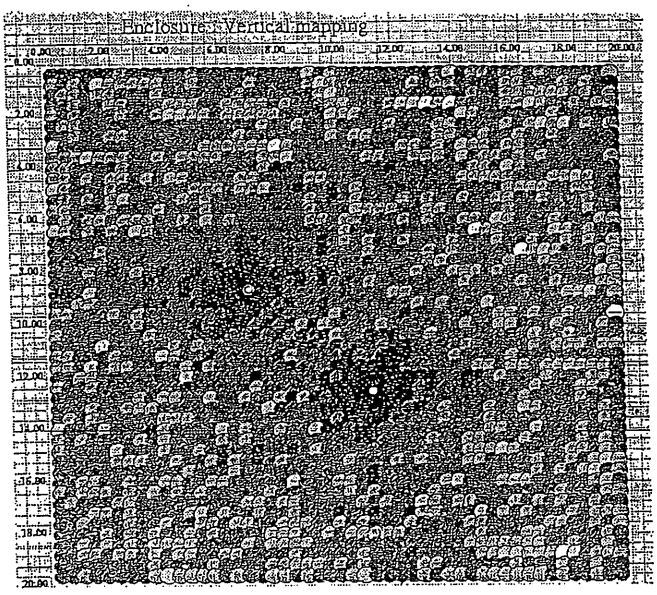

Figure 9. Sound field when a secondary monopole is far from the primary source

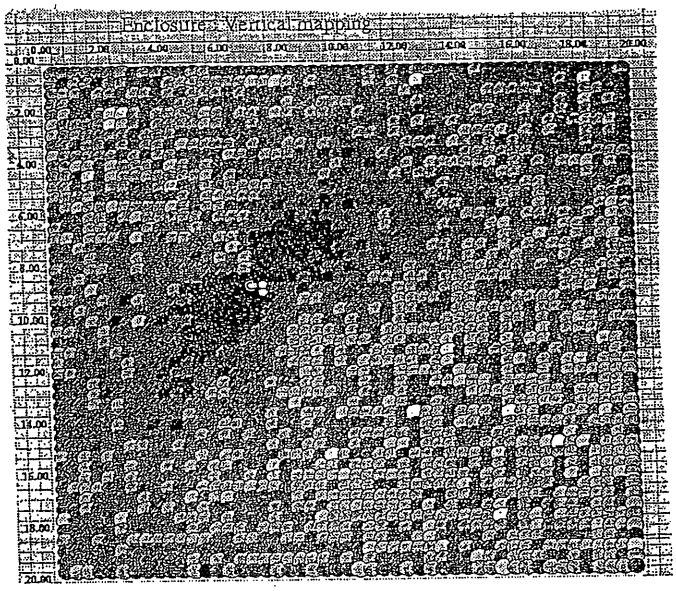

Figure 10. Sound field when a secondary dipole is close to the primary source

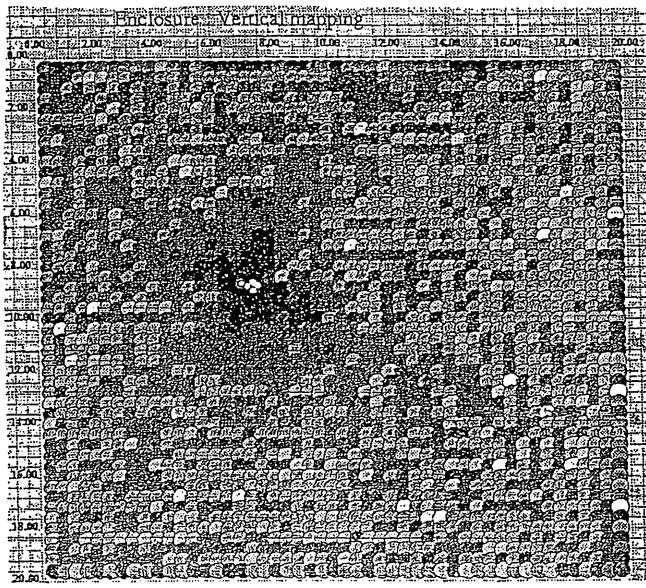

Figure 11. Sound field when a secondary quardrupole is close to the primary source

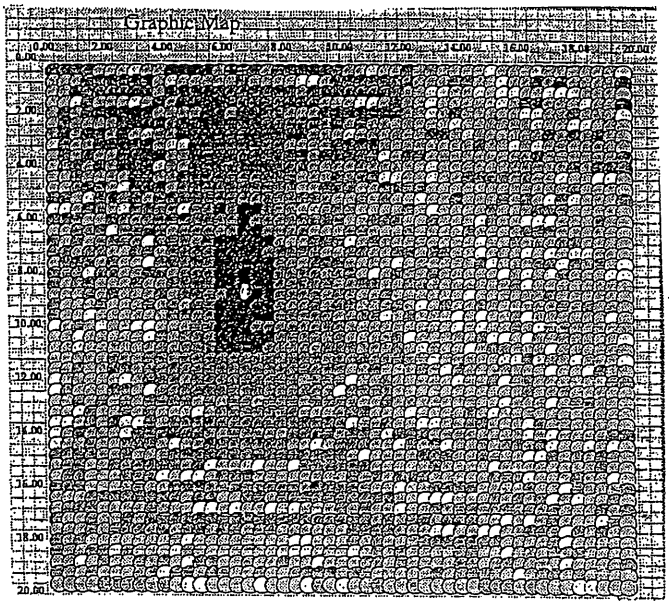

Figure 12. Sound field when two secondary monopoles of half the strength of the primary source each are close to the primary source

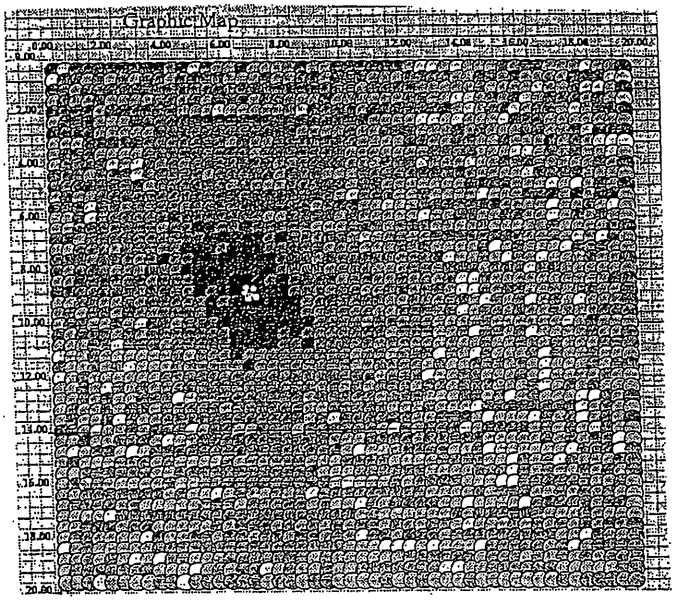

Figure 13. Sound field when five secondary monopoles of fifth the strength of the primary source each are close to the primary source